Synthesis, Characterization, and Properties of Novel Polyisobutylene-Based Urethane Model Networks

J. P. KENNEDY and J. LACKEY*, *Institute of Polymer Science, University of Akron, Akron, Ohio 44325*

Synopsis

This paper concerns the synthesis, characterization, and physical properties of novel polyisobutylene (PIB)-based urethane model networks prepared from diphenylmethane diisocyanate (MDI) and three-arm star PIBs capped with $-CH_2OH$ end groups ($PIB(CH_2OH)_3$). The $PIB(CH_2OH)_3$ starting materials were produced by the inifer method in the $\bar{M}_n$ = 13,550–27,000 range. The best networks were obtained with NCO : OH = 1. Solvent extractions showed uncatalyzed network formation to be essentially complete and swelling studies indicated the expected architecture, i.e., $\bar{M}_c = 2\bar{M}_n/3$ and virtual absence of dangling chains. Stannous octoate was found to increase the rate of network formation in the absence of side reactions (i.e., allophanate formation), while other catalysts also accelerated undesirable reactions. The effect of molecular weight between crosslinks ($\bar{M}_c$) on network physical properties has been studied in the $\bar{M}_c$ = 900–18,500 range. The tensile strength increases with decreasing $\bar{M}_c$ up to a limiting value after which it sharply declines. Elongations at break decrease monotonously with decreasing $\bar{M}_c$. Low temperature tensile studies show higher tensile data at −20°C, and, surprisingly, a retention of elongations at break. The T_g's decrease with increasing $\bar{M}_c$'s until a plateau is reached at −73°C. Hysteresis is fairly constant and permanent set is constant and low. The PIB-based urethane networks exhibit excellent hydrolytic stability, negligible moisture absorption, and outstanding heat-aging stability, far beyond what is expected for a polyurethane. Conceivably the thermal deblocking of the urethane group may be reversible ($-NH-COO-CH_2- \rightleftharpoons -NCO + HOCH_2-$) because the isocyanate that arises in the highly hydrophobic PIB matrix recombines with the alcohol, and cannot react with moisture as in conventional urethane networks.

INTRODUCTION

The design of polymeric materials with specific desirable properties demands the controlled synthesis of well-defined polymer structures. Precisely defined networks, i.e., model networks, may be obtained by end-linking linear or three-arm star prepolymers capped with a suitable functional group (e.g., $-CH_2OH$) and a tri- or bifunctional crosslinker (e.g., isocyanate), respectively. Previous work from this laboratory described model polyurethane networks prepared by the first route, i.e., by reacting linear polyisobutylenes (PIB) capped by $-CH_2OH$ with a triisocyanate.[1] The present study concerns model PIB-based urethane networks obtained by the use of three-arm star PIBs carrying $-CH_2OH$ end groups ($PIB(CH_2OH)_3$) crosslinked with a diisocyanate.

Recent fundamental studies into the mechanism of isobutylene polymerizations gave rise to the inifer technique which led to the controlled synthesis

*Present address: Dow Chemical Co., Freeport, TX 77541.

Journal of Applied Polymer Science, Vol. 33, 2449–2465 (1987)

CCC 0021-8995/87/072449-17$04.00

of well-defined liquid linear and three-arm star PIBs carrying *tert*-chlorine end groups.[2,3] By suitable quantitative modifications these precursors have been converted into a great variety of telechelic (terminally functional) intermediates, including PIB-diols and -triols.[4,5]

Model networks of well-defined PIB strands crosslinked by isocyanates are valuable substances for the exploration of theories of rubberlike elasticity.[1,6,7] Since molecular weight control of alcohol-telechelic PIBs can be readily accomplished[4,5] and the crosslinking of PIB-diols or -triols with isocyanates is essentially quantitative, the possibility for the synthesis of model networks arises. In these model rubbery networks the average molecular weight between crosslinks, $\overline{M}_c$, is a simple function of the $\overline{M}_n$ of the starting materials, i.e., $\overline{M}_c \approx \overline{M}_n$ for linear PIB-diols crosslinked with triisocyanates[1] and $\overline{M}_c = 2\overline{M}_n/3$ for three-arm star PIB-triols crosslinked with diisocyanates. The placement of functional groups exclusively at the chain ends yields networks with negligible "dangling chains."

PIB-based urethane networks are also of great practical interest as they combine the excellent physical–mechanical–chemical properties of the PIB chain (low T_g, excellent environmental resistance, outstanding barrier properties, etc.) with the advantages of a polyurethane.[8–10]

This paper concerns the synthesis of model polyurethane networks from $PIB(CH_2OH)_3$ and MDI, characterization research to demonstrate complete crosslinking, and physical property studies to illustrate some desirable features of PIB-based polyurethanes.

EXPERIMENTAL

Materials

Three-arm star polyisobutylene triols were synthesized by the tricumyl chloride trinifer as described.[5] The tricumyl chloride was purified by repeated crystallizations and its purity was ascertained by ^{1}H-NMR spectroscopy, thin layer chromatography, and melting point T_m = 68–69°C measurements.

4,4-Diphenylmethane Diisocyanate (MDI) (95–98%, Mobay Chemical Co.) was stored in a freezer and was vacuum-distilled under dry N_2 at ~ 1 mm Hg, utilizing a short path distillation set immediately prior to use. The MDI began to distill at 180°C; the pure middle fraction was a white crystalline solid, M_p = 38°C, and was used within 2 h of distillation. According to standard titration (i.e., addition of di-*n*-butyl amine followed by back-titration with acid), the NCO content of the purified MDI was essentially theoretical.

m-Xylene used in network synthesis was distilled over sodium immediately prior to use.

Benzene and n-Pentane used in swelling and extraction studies were used as received.

CHARACTERIZATION METHODS

Vapor Pressure Osmometry (VPO). Number average molecular weights were determined by using a Knauer Model No. 11.00 vapor pressure osmometer and toluene (distilled over calcium hydride) at 40°C. Great pains were

taken to purify the samples since low molecular weight impurities would greatly reduce the measured molecular weight values. Thus a 20% polymer solution in hexane was precipitated into a 4 : 1 methanol/acetone mixture, the precipitate filtered, redissolved in hexane, washed with distilled water, dried over anhydrous magnesium sulfate, filtered, and the solvent removed. To remove the last traces of hexane, the dried polymer was redissolved in dry toluene, the solvent removed, the polymer redissolved, and the toluene again removed. The sample was then dried in a vacuum oven at 80°C for 1 week. Four different polymer solutions, 10–100 g/kg, dry toluene were used for each run. The VPO was calibrated using zone purified biphenyl and recrystallized sucrose acetate.

Gel Permeation Chromatography (GPC). The system consisted of a Waters 6000A pump, a Waters R401 differential refractometer, a Waters 440 UV detector and five Waters μ-Styragel columns with pore sizes of 100, 500, 10^3, 10^4, and 10^5 Å. The mobile phase (dry THF) was pumped at 1 mL/min. The samples were 0.25–0.40% (w/w), depending on the molecular weight of the polymer. The samples were prepared in the same THF as the mobile phase. A calibration curve was constructed using a series of PIB standards of known molecular weights. The calibration was checked periodically.

Differential Scanning Calorimetry (DSC). A DuPont 990 Thermal Analyzer was used. Each sample was scanned at 20, 10, and 2°C/min, and the T_g was taken from the extrapolated zero scan rate.

Infrared Spectroscopy (IR). IR was run on a Perkin-Elmer Model 521 using 1 mm thick films. Hydroxyl functionality was determined by the use of a pair of Barnes 50 mm long path cells with sodium chloride windows.

Ultraviolet Spectroscopy (UV). A Perkin-Elmer Model 559A UV/VIS spectrophotometer was used. A typical sample was made by dissolving 25 mg $PIB(CH_2OH)_3$ in 5 mL of spectro grade *n*-hexane.

Physical Testing Methods. An Instron Tabletop model tensile tester was used. A cooling chamber connected to a Dewar container filled with liquid nitrogen was used for measurements at −20°C. Dynamic stress–strain experiments were carried out using 5 × 0.25 × 0.2 cm microdumbbells under continuous strain at 2 in./min.

Hysteresis loops were generated at a constant rate of 2 in./min to a strain of ~ 80% of strain at break. As samples reached 80% of strain at break, the crosshead direction was reversed, and run at the same speed until the stress reached zero. The strain was measured at this point and used to determine the permanent set of the material.

Air oven aging was carried out according to ASTM-D537. Microdumbbells were suspended in a circulating air oven for 48 h at 128°C, then cooled to room temperature, and the tensile properties measured. The percent change in tensile strength from the pretest values were determined.

Hydrolytic stability was determined by ASTM-D3137. Samples were suspended in distilled water for 96 h at 85°C, cooled to room temperature, and dried, and tensile properties were measured as above.

Water absorption was determined by ASTM-D570. Samples were submersed in distilled water at 70°C for 48 h, then the surface water was blotted off, and the samples were weighed immediately. The weight gain as a percentage of the original weight was calculated.

Swelling and Extraction

A preweighed 2 × 2 × 0.3 cm sample was submerged at room temperature in either *n*-pentane or benzene in a glass dish with a lid. After 24 h the swollen sample was blot-dried, transferred to a dry, closed dish, and weighed. The sample was then placed in fresh solvent, and the procedure repeated until equilibrium swollen weight was obtained. At this point the sample was dried under vacuum and the equilibrium dry weight was determined. A minimum of three samples were averaged (including weights for swelling ratio and polymer density).

Degradative Oxidation of Central Phenyl Ring

Aqueous 30% H_2O_2 (24 mL) in trifluoroacetic acid (1 : 5, v/v) was dripped into a stirring solution of 1% polyisobutylene in 50 mL CCl_4 and the system heated to reflux. Periodically, samples were removed from the water layer and titrated with KI solution to ensure the presence of peroxide. A small (1–2 mL) amount of H_2O_2–trifluoroacetic acid was added if the test was negative. Occasionally samples of the CCl_4 layer were removed, and the polymer was isolated to be examined by GPC (see above). IR was run as described above, and the observation of the absorbance peak at 1760^{-1} cm characteristic of the C=O of the carboxylic acid was noted.

Functionality Determination of Isocyanates

A standard amine titration was employed to determine the functionality of isocyanates. The isocyanates were reacted with an excess of di-*n*-butylamine, then titrated with a standard 0.5*N* HCl solution. Since a known amount of amine was added, the amine no longer present is assumed to have reacted completely with the isocyanates and the amount of isocyanate present can be determined.

Experimentally, ~ 10 g of isocyanate were dissolved in rigorously dried toluene, 40 mL of 2*N* di-*n*-butylamine were added, and the system was refluxed. The system was cooled to room temperature and ~ 200 mL of methanol were added. Bromophenol blue indicator was added, and the solution was titrated with the HCl solution. The results of three titrations were averaged. A blank was run along with each set of titrations.

The percent isocyanate was calculated by the following equation:

$$\% \text{ NCO} = \{[(R - S) \times N/1000 \times E]/\text{W}\} \times 100$$

where R = mL HCl consumed by the blank, S = mL HCl consumed by the sample, N = normality of acid, E = theoretical equivalent weight of isocyanate, and W = sample weight.

A compound with theoretical functionality would yield a % NCO of 100, a compound with half the theoretical functionality would yield a % NCO of 50, etc.

NETWORK SYNTHESIS

Network syntheses were performed in a stainless steel enclosure under a dry (BaO) nitrogen atmosphere. The $PIB(CH_2OH)_3$ was weighed into a beaker and a minimum amount (< 5% of PIB weight) of dry xylene was added to render

the polymer pourable. MDI preweighed in a glass vial and dissolved in dry xylene was added to the PIB triol at room temperature, and the system stirred thoroughly with a glass rod. In experiments with catalyst (1–3 phr), the catalyst was added with the MDI. The mixtures were then poured into Teflon molds floating on a bed of mercury. The systems containing catalyst were cured in the dry box for 24 h and then further cured in an oven under N_2 for an additional 24 h at 45°C. Systems without catalyst were cured for 1 week at room temperature in the dry box and for an additional 3–7 days in an oven under N_2 at 85°C. The optimum NCO : OH ratio was determined by extraction studies to be 1 : 1. Clear colorless or slightly yellow elastic films were obtained.

RESULTS AND DISCUSSION

Characterization of $PIB(CH_2OH)_3$

The synthesis of $PIB(CH_2OH)_3$ has been carried out by the tricumyl chloride trinifer[5] followed by quantitative conversion of the *tert*-chlorine precursor to the alcohol.[3] The structures of the products were investigated by a battery of methods including ^{1}H-NMR, UV, and quantitative IR spectroscopies, and oxidation and fragment analysis:

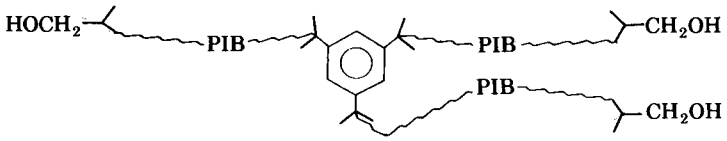

$PIB(CH_2OH)_3$

The ^{1}H-NMR analysis of this PIB triol has already been published[5]; however, the low sensitivity of 60 MHz spectroscopy was insufficient for routine analysis, particularly in view of the needed very high structural purity of the prepolymers.

UV spectroscopy was found to be sufficiently sensitive for the analysis of the possible presence of very low concentrations of "unfired" trinifer groups in the precursor. The analytical task was to distinguish between the following precursor termini:

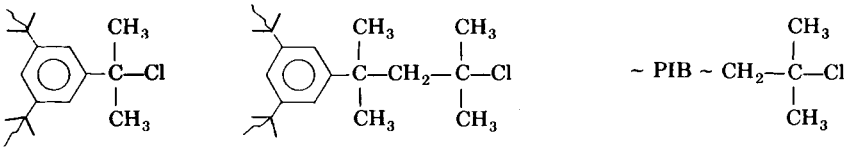

Unfired end group "Once-fired" end group Desired end group

Experimentally, we treated our products by the strong base tBuOK quantitatively to convert the *tert*-chlorine groups to the corresponding exo-olefins and analyzed the UV spectra of the dehydrochlorinated products:

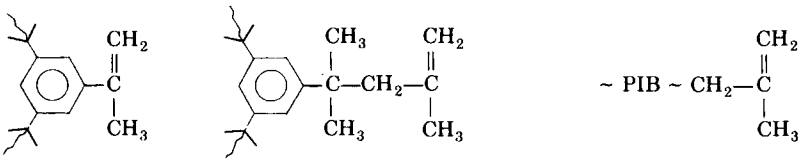

The presence of unfired groups would have been detected by a strong UV absorption due to the conjugated nature of the structure. In fact, in no case did we encounter a strong UV absorption indicative of a conjugated structure, i.e., unfired end groups were virtually absent. The spectra for the *tert*-chlorine precursor and those of the dehydrochlorinated products were essentially undistinguishable suggesting the absence of conjugation. Figure 1 shows a representative spectrum of (a) the starting material, (b) the starting material after dehydrochlorination, and (c) the starting material to which a small amount of 1,3,5-triisopropenylbenzene (5 mol %) was added. The purpose for the addition of the 1,3,5-triisopropenylbenzene model compound was to mimick the UV absorption of the unfired/dehydrohalogenated structure.

The possible presence of once-fired termini has been ruled out by directly determining the number of PIB arms emanating from the central aromatic ring (trinifer residue). Experimentally, we selectively degraded (oxidized) the central phenyl moiety and determined the molecular weights and molecular weight distributions before and after the degradative oxidation step. According to these measurements, upon degradative oxidation the $\bar{M}_n$ of the products decreased by a factor of 3 with the dispersities remaining essentially unchanged. Figure 2 and Table I show the data. The authors who developed this selective ring cleavage method[11] observed that CF_3COOOH oxidation of the central phenyl ring gives rise to carboxylic acids. We have corroborated this by independent IR spectroscopy. According to these studies the $PIB(CH_2OH)_3$ is radial in nature with three PIB chains per molecule.

The number average terminal functionality $\bar{F}_n$ of the $PIB(CH_2OH)_{33}$ products was determined by quantitative IR spectroscopy coupled with $\bar{M}_n$ determination.[12] This method is routinely used to determine $\bar{F}_n$ of PIB-diols and -triols in our laboratory. Table II shows the $\bar{F}_n$ values of some representative $PIB(CH_2OH)_3$s: Evidently, $\bar{F}_n = 3.0 \pm 0.06$; the experimental error of the method is $\pm 5\%$.

According to these various independent studies, the microarchitecture of the $PIB(CH_2OH)_3$ starting materials has been satisfactorily defined: They comprise a central phenyl ring (inifer residue) carrying three PIB chains capped by a $-CH_2OH$ end group. Evidence for unfired and/or once-fired end groups has not been found. The possibility for the formation of indanyl end groups in tricumyl chloride trinifer systems has been excluded.[5,13,14] The

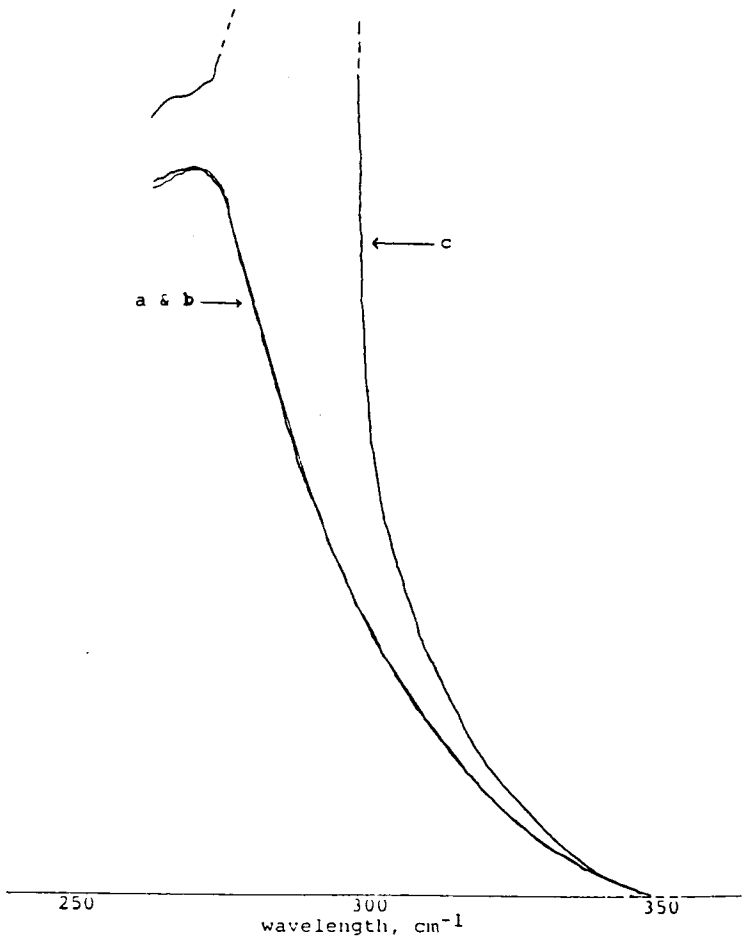

Fig. 1. UV spectrum of: (a) chlorine-terminated three-arm star polyisobutylene; (b) olefin-terminated three-arm star polyisobutylene; (c) (b) plus 5% (molar) 1,3,5-triisopropenyl benzene.

overall molecular weights of the products can be readily controlled by the [monomer]/[trinifer] ratio in the carbocationic synthesis step.

NETWORK SYNTHESIS

After having ascertained that both starting materials, $PIB(CH_2OH)_3$ and MDI, were well defined and characterized, research was carried out to work out conditions conducive for model network formation.

OH : NCO Ratios

We set out to determine the optimum OH : NCO ratio, i.e., the $PIB(CH_2OH)_3$: MDI molar ratio yielding the least amount of extractables. Thus series of networks have been synthesized by varying the OH : NCO ratio (i.e., 0.9/1.0, 0.95/1.0, 1.0/1.05, 1.0/1.1, etc.); however, the best networks (in terms of % extractables) were invariably obtained with OH : NCO = 1.0.

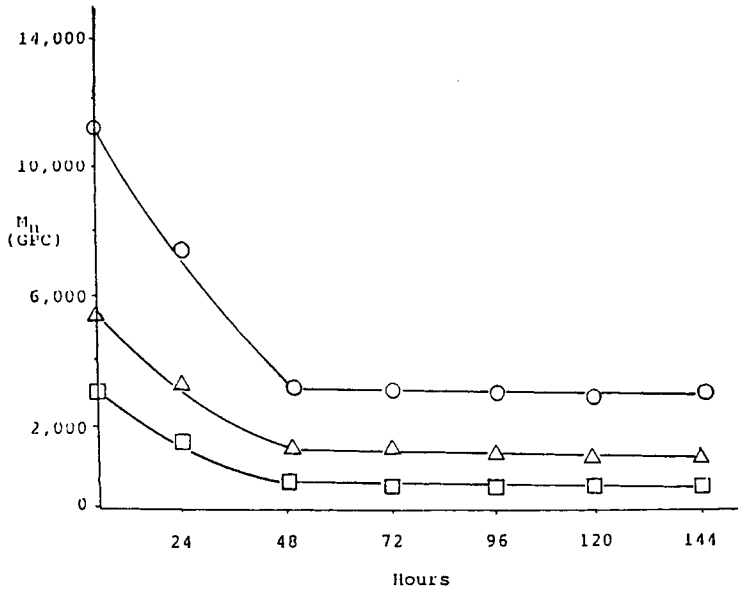

Fig. 2. Results of central ring cleavage of three-arm PIB using trifluoroperacetic acid. $\bar{M}_n$: (○) 11,200; (△) 5400; (□) 3000.

TABLE I
Results of Oxidative Degradation of Aromatic Ring in Three-Arm Star Telechelic Polyisobutylenes

Original		After degradation		
$\bar{M}_n$ [a]	$\bar{M}_w/\bar{M}_n$ [a]	$\bar{M}_n$ [a]	$\bar{M}_w/\bar{M}_n$ [a]	$\bar{M}_n$ (orig)/$\bar{M}_n$(degr)
11,200	1.51	3330	1.48	3.36
5400	1.46	1540	1.49	3.50
3000	1.44	950	1.50	3.14

[a] Determined by GPC, based upon calibration utilizing PIB standards.

TABLE II
Hydroxyl Functionality of Three-Arm Star Telechelic Polyisobutylenes as Determined by IR Spectroscopy

PIB–$(CH_2OH)_3$ $\bar{M}_n$ [a]	Hydroxyl eq wt (g/mol OH)	$\bar{F}_n$ [b]
11,600	3910	2.96
5600	1830	3.06
3100	1050	2.95
1350	460	2.94

[a] By VPO.
[b] $\bar{M}_n$/hydroxyl eq wt.

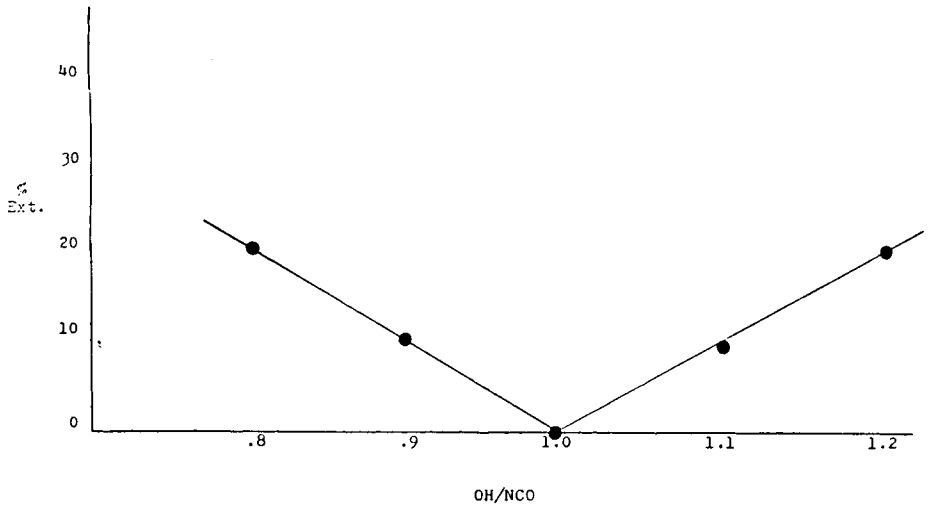

Fig. 3. Sol fraction vs. OH : NCO ratio, $\overline{M}_n$ = 5600.

Figure 3 shows the results of a representative series of experiments with the $\overline{M}_n$ = 5600 PIB$(CH_2OH)_3$.

The effect of OH : NCO was further investigated by IR spectroscopy. According to these studies the absorption at 2300 cm^{-1} due to free —NCO groups is absent in films prepared with OH : NCO = 1.0, whereas a strong absorption can be seen when the molar ratio is less than unity. Figure 4 compares the IR spectra for PIB-based urethanes: one prepared with OH : NCO = 1.0 another with OH : NCO = 0.8. These studies corroborate the results of extraction experiments and further demonstrate the purity of the

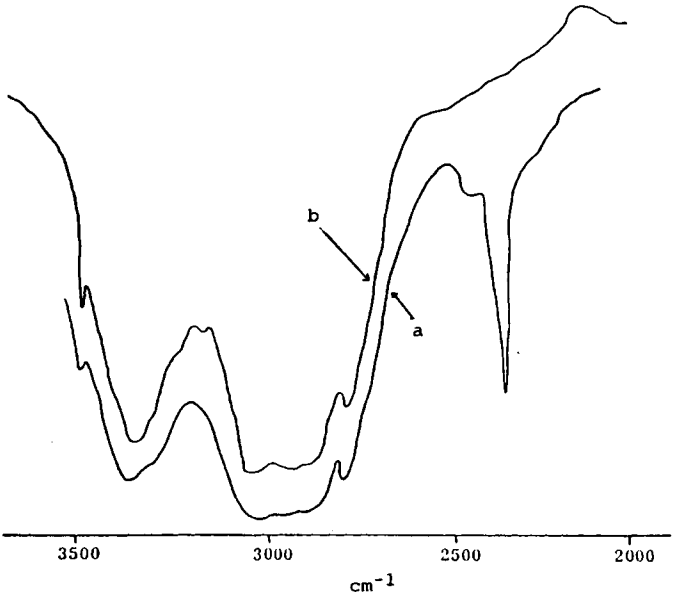

Fig. 4. IR spectra of PIB–urethane made with: (a) OH/NCO = 0.8; (b) OH/NCO = 1.0.

starting materials. The lack of a strong peak at 1650–1700 cm^{-1}, characteristic of the allophanate group, indicates the absence of such groups.

NETWORK CHARACTERIZATION

Swelling Studies

Characterization has centered on networks prepared from five PIB(CH_2OH)$_3$s with $\overline{M}_n$'s = 27,700, 11,600, 5600, 3100, and 1350. (The $\overline{M}_n$'s were determined by VPO except the highest $\overline{M}_n$ triol, which was characterized by GPC.) The corresponding theoretical $\overline{M}_c$'s of the networks should be $2\overline{M}_n/3$, i.e., 18,500, 7730, 3730, 2070, and 900.

Experimentally M_c's were determined by swelling measurements according to Flory and Rehner.[15] Accurate weights were obtained to calculate the swelling ratio. Table III shows the $\overline{M}_c$ results together with extraction data. Evidently, the experimental data closely approach the theoretical values indicating complete "clean" endlinking free from undesired side reactions (e.g., allophanate formation which would tend to result in smaller than theoretical $\overline{M}_c$ values).

This conclusion is substantiated by the results of extraction studies which show negligible sol fraction; see the data included in Table III. The extractions were performed by benzene (data in Table III), *n*-pentane, and THF to make sure that the low sol fractions were not due to the use of one specific solvent. The essential absence of soluble matter indicates the completeness of the network forming reactions.[16]

Catalyst Studies

In view of the rather long time requirement of the end-linking (curing) reaction, efforts have been made to accelerate the curing by the use of catalysts known to promote urethane formation. Table IV shows the catalysts used and the $\overline{M}_c$ calculated from swelling data. Interestingly, curing in the absence of catalyst and with stannous octoate gave close to theoretical $\overline{M}_c$'s, indicating clean end-linking reactions. In the presence of this tin compound, curing time was reduced from 2 weeks to 2 days, and the curing temperature

TABLE III
Network Characterization by Swelling and Extraction

$\overline{M}_n$ PIB–(CH_2OH)$_3$	$\overline{M}_c$			Solvent extractable (%)	
	Theory	Swelling in benzene	Swelling in *n*-pentane	Benzene	*n*-Pentane
27,000[a]	18,500	16,850	19,600	1.4	2.4
11,600[b]	7730	6800	8120	0.8	0.2
5600[b]	3730	3200	3500	0.8	0.5
3100[b]	2070	1820	2150	0.4	0.2
1350[b]	900	810	820	0.7	0.6

[a]GPC.
[b]VPO.

TABLE IV
Effect of Catalyst on Network Structure

Catalyst	$\bar{M}_c$	
	Theo	Exptl (from swelling[a])
None	7700	6800
	2100	1820
Dibutyltin dilaurate	7700	3450
	2100	990
Triethylene diamine	7700	3110
	2100	910
Stannous octoate	7700	7230
	2100	1920

[a] In benzene.

from 85 to 45°C. In contrast, dibutyltin dilaurate and triethylene diamine consistently yielded much lower than expected $\bar{M}_c$ values (higher moduli), i.e., higher than expected crosslink densities. We construe this to be due to allophanate crosslink formation. The reason why stannous octoate would yield a cleaner reaction than the other tin catalyst is obscure, although the effect has also been noted by others.[17]

Tensile Studies

Figure 5 and Table V show the results (averages of three to five experiments). To facilitate internal comparisons (and less to compare our materials with commercial products) the strengths are expressed in terms of true stresses rather than engineering stresses. The tensile strength increases with

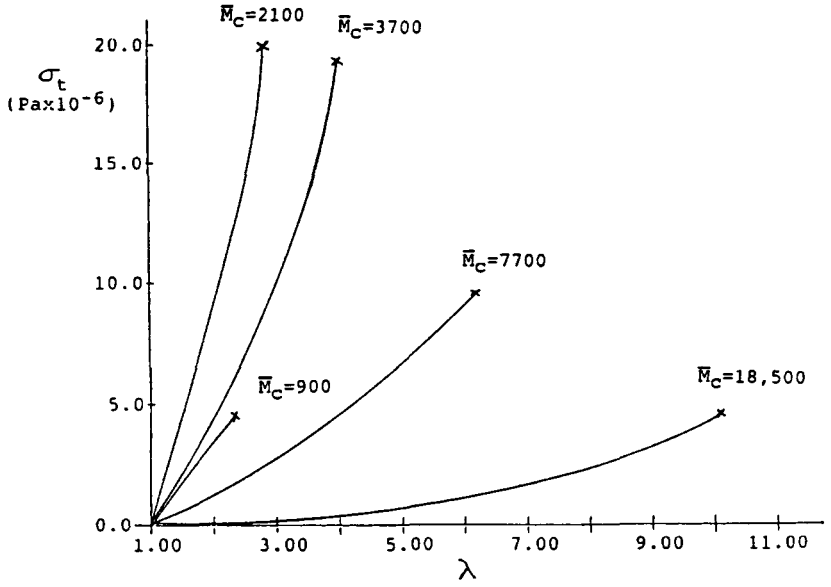

Fig. 5. Stress–strain curves of polyisobutylene-based urethane networks.

TABLE V
Tensile Strength and Ultimate Elongation of PIB–Urethanes

$\bar{M}_c$ [a]	True stress at break (Pa)[a]	Elongation at break (%)[b]
900	4.84×10^6	140
2100	1.85×10^7	227
3700	1.81×10^7	300
7700	9.40×10^6	510
18500	4.11×10^6	1010

[a] Based on $\bar{M}_n$ of prepolymer.
[b] Strained at constant rate of 2 in./min.

TABLE VI
Tensile Properties of PIB–Urethanes at −20°C

$\bar{M}_c$ [a]	$\sigma_{t,b}$ (Pa)[b]	Change relative to 25°C results (%)	E_b(%)[b]	Change relative to 25°C results (%)
900	2.31×10^6	−52	1	−100.0
2100	2.66×10^7	44	233	2.6
3700	2.61×10^7	45	289	−3.7
7700	2.55×10^7	170	530	3.9
18500	5.20×10^6	27	1000	−1.0

[a] Based on prepolymer $\bar{M}_n$.
[b] At −20°C, at a constant strain rate of 2 in./min.

decreasing $\bar{M}_c$ in the $\bar{M}_c$ = 18,500–2100 range; however, then it drops precipitously at $\bar{M}_c$ = 900. This phenomenon may be explained by assuming at least two scenarios (or by a combination of at least two scenarios):

In a real rubber the distribution of stresses borne by different chains varies widely. Since the chains are crosslinked in their random-coil state, some chains will be relaxed when incorporated into the network, while others will be in a highly extended state. Also, since few polymer samples are truly monodisperse, some chains will be much shorter than others. Upon stretching, the shorter chains will be elongated first and will therefore break first. Beuche[18] showed that the effects of the uneven distribution of load among the chains of the network is more pronounced at high degrees of crosslinking (low $\bar{M}_c$) than at low degrees of crosslinking (high $\bar{M}_c$). The ratio of the extended chain length of a freely oriented chain to its random length is $N^{1/2}$, where N is the number of freely orienting segments per chain. The pronounced effect at high crosslinking is a result of the fact that the percent deviation from the average for the number of segments per network chain increases as the number of segments per average chain decreases. Therefore, when the network chains contain on average only a few segments, the chance of finding a chain with only half the average number of segments is greater than if the average chain contained a large number of segments. As a result, the number of highly stressed chains increases as the degree of crosslinking increases.

According to Bueche,[18] a sample fails when the stress causes a chain to break, which causes another chain to break, etc., resulting in catastrophic failure. When a chain breaks, the load it was bearing must be assumed by its

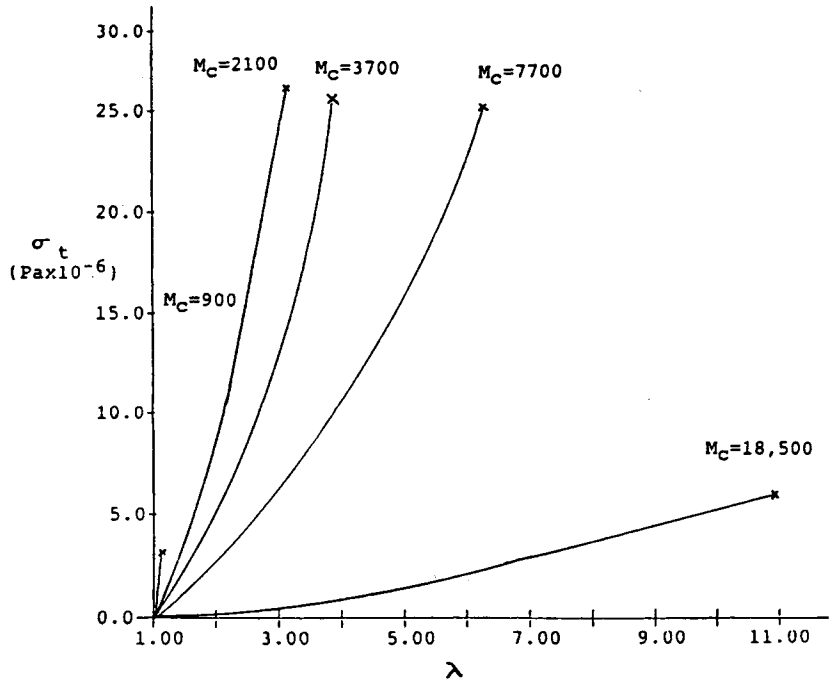

Fig. 6. Low temperature (−20°C) stress–strain plots of polyisobutylene-based urethane networks.

neighboring chains. If one of these chains is already highly stressed, the chances of it failing are high. If the number of highly stressed chains in the network is higher, as in the case of the very low $\bar{M}_c$ network, then it will be relatively easier to break it. Thus, too high a crosslink density will result in a wide distribution of stresses which in turn will lead to a drop in tensile strength.

A second explanation for the observed effect may be related to the ratio of urethane groups to the PIB chains in the network. At high $\bar{M}_c$'s the relative number of urethane groups is low, i.e., the network is a moderately crosslinked PIB network. As the $\bar{M}_c$ is increased, the relative amount of urethane groups is increased, leading to an increase in tensile strengths due to hydrogen bonding between urethane groups, while still retaining the flexibility of the PIB chains. At the extreme of $\bar{M}_c = 900$, very little PIB character remains; the network becomes a highly crosslinked brittle urethane; thus a sharp drop in tensile strength occurs.

Figure 6 and Table VII show stress-strain values determined at −20°C. The elongation remained relatively unchanged from the values at room temperature, with the exception of the $\bar{M}_c = 900$ sample, which exhibited a sharp, 100% drop in elongation. The latter observation reflects the usual effect of temperature on moduli: Lowering the temperature is equivalent to increasing the strain rate which reduces the ability of chains to rearrange and to accommodate the increasing stresses as the sample is elongated. The relative insensitivity of the elongations of the other networks is more difficult to

TABLE VII
Hysteresis of PIB–Urethanes

$\bar{M}_c$ [a]	Strain energy lost (%)[b]	Permanent set (%)[b]
900	24	6
2100	33	4
3700	20	6
7700	26	11

[a] Based on prepolymer $\bar{M}_n$.
[b] From hysteresis loop generated at constant rate of 2 in./min to strain of ~ 80% of strain at break.

explain. Conceivably, the strength of hydrogen bonding between urethane groups may increase with decreasing temperatures.

The tensile strength of the networks is higher at −20°C, except the $\bar{M}_c$ = 900 sample, which exhibits anomalous behavior relative to the other samples. This effect has been expected since the lowering of the temperature is equivalent to an increasing of the strain rate. At higher temperatures the chain segments are able to respond rapidly to the imposed stress and reach full elongation. At this point each chain contributes just once to the load bearing of the stressed system. At lower temperatures the time frame is too short for the chains to fully elongate; many of the motions are frozen out, and some of the entangled chains may supply more than one bond to the load-bearing process. This results in higher tensile strengths, and indeed has been observed in four of the five samples.

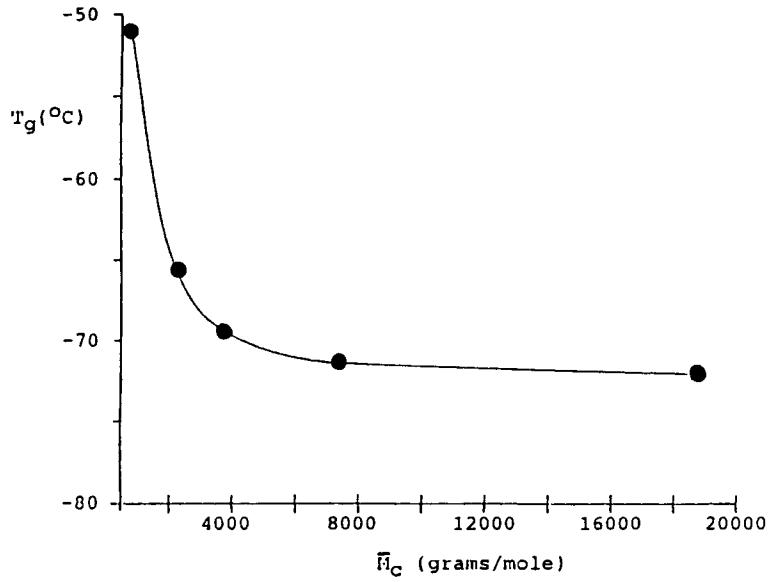

Fig. 7. Effect of $\bar{M}_c$ on T_g.

Structure–T_g Effect

Figure 7 shows the results. Increasing the extent of crosslinking increases the glass transition temperature by reducing the mobility of the chains. At a sufficiently high $\overline{M}_c$, the T_g reaches that of PIB, i.e., ~ −73°C. Beyond this $\overline{M}_c$, the T_g remains the same, as expected.

Hysteresis Studies

The hysteresis loops of PIB-based urethane networks have been examined to study recovery characteristics as a function of $\overline{M}_c$. Figure 8 and Table VII show the results. The samples were strained at a constant rate to 80% of their strain-at-break values. The strain energy lost during deformation was found to remain relatively constant, i.e., ~ 26%. The constancy of these values suggests network uniformity, i.e., absence of dangling chain ends.

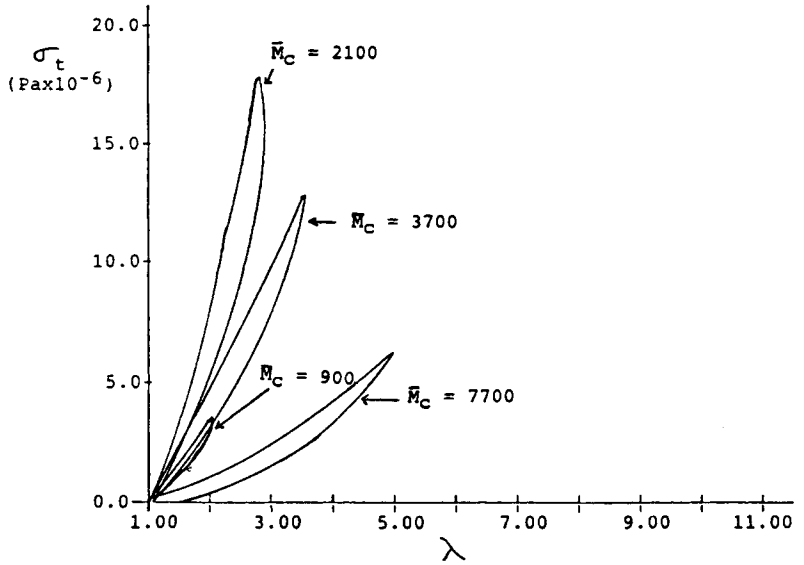

Fig. 8. Hysteresis loops of PIB-based urethane networks.

TABLE VIII
Hot Water and Hot Air Resistance of PIB-Based Polyurethanes

	Before degradation testing		After exposure to hot water[b]			After air-oven aging[c]		
$\overline{M}_c$[a]	$\sigma_{t,b}$ (Pa)	E_b (%)	$\sigma_{t,b}$ (Pa)	E_b (%)	Change in $\sigma_{t,b}$ (%)	$\sigma_{t,b}$ (Pa)	E_b (%)	Change in $\sigma_{t,b}$ (%)
2100	1.85×10^7	227	1.76×10^7	222	−4.86	1.81×10^7	224	−2.16
3700	1.81×10^7	300	1.73×10^7	298	−4.42	1.76×10^7	290	−2.76
7700	9.40×10^6	510	9.34×10^6	492	−0.64	9.11×10^6	494	−3.09

[a] Based on M_n of prepolymer.
[b] ASTM-D3137.
[c] ASTM-D537.

Permanent set (residual strain remaining after relieving the stress) also remained relatively constant, i.e., ~ 6.7%. Conceivably the constancy in hysteresis loss and permanent set may be due to the same structural factors (lack of significant network imperfections); otherwise, the range of structural variations would be insufficient to induce significant changes in hysteretic properties.

Moisture Absorption, and Hot Water (Hydrolytic) and Hot Air Resistance

In view of the hydrophobic and saturated nature of PIB rubbers, we expected our PIB-based urethane networks to exhibit outstanding environmental resistance, i.e., low moisture absorption, high hydrolytic, and hot air (oxidative) resistance. Table VIII shows representative results. The hydrolytic stability was obtained by determining the room temperature tensile properties of samples before and after immersing them in distilled water at 85°C for 96 h. The loss in properties is expressed as the percent change. Similarly, oxidative stability was measured by determining the percent loss in tensile properties of samples before and after exposure to 128°C in a circulating air oven for 48 h. According to the data displayed in Table VIII, the loss in properties in the hydrolysis and hot air tests were negligible; indeed the changes in properties were essentially within experimental variation. Similarly, moisture absorption (measured by submerging preweighed samples in water at 75°C for 48 h, removing them, and blotting off surface water) was also found to be negligible, i.e., 0.0% within experimental error.

Excellent hydrolytic resistance and zero moisture absorption are due to the highly hydrophobic nature of the networks. The outstanding thermal resistance is more surprising since it is determined by deblocking of the urethane groups and less by the nature of the flexible segment. A possible explanation for the lack of thermal degradation under the test conditions may be due to the absence of traces of moisture in the highly hydrophobic PIB matrix. In conventional (polyester-, polyether-based) urethanes, deblocking to isocyanate and alcohol groups may be immediately followed by reaction of the —NCO function with traces of moisture present in the polar matrix:

$$\sim \text{NH—COO} \sim \rightarrow \sim \text{NCO} + \text{HO} \sim \xrightarrow{\text{H}_2\text{O}} \sim \text{NH—COOH} + \text{HO} \sim$$

In the highly hydrophobic PIB network, deblocking may be reversible because of the absence of traces of moisture. In a sense this phenomenon is reminiscent of the "cage effect."

This material is based upon work supported by the National Science Foundation (Grant DMR-84-18617). We gratefully acknowledge criticism and advice by F. N. Kelley and J. E. Mark.

References

1. T. Miyabayashi and J. P. Kennedy, *J. Appl. Polym. Sci.*, **31**, 2523 (1986).
2. J. P. Kennedy and R. A. Smith, *J. Polym. Sci., Polym. Chem. Ed*, **18**, 1539 (1980).
3. J. P. Kennedy, V. S. C. Chang, R. A. Smith, and B. Iván, *Polym. Bull.*, **1**, 575 (1979).

4. B. Iván, J. P. Kennedy, and V. S. C. Chang, *J. Polym. Sci., Polym. Chem. Ed.*, **18**, 3177 (1980).
5. J. P. Kennedy, L. R. Ross, J. E. Lackey, and O. Nuyken, *Polym. Bull.*, **4**, 67 (1981).
6. P. H. Sung, S. J. Pan, J. E. Mark, V. S. C. Chang, J. E. Lackey, and J. P. Kennedy, *Polym. Bull.*, **9**, 375 (1983).
7. J. E. Lackey, V. S. C. Chang, J. P. Kennedy, Z. M. Zhang, P. H. Sung, and J. E. Mark, *Polym. Bull.*, **11**, 19 (1984).
8. V. S. C. Chang and J. P. Kennedy, *Polym. Bull.*, **8**, 69 (1982).
9. V. S. C. Chang and J. P. Kennedy, *Polym. Bull.*, **9**, 479 (1983).
10. J. P. Kennedy and J. E. Lackey, *Polym. Mater. Sci. Eng.*, **49**, (1983).
11. V. S. C. Chang, J. P. Kennedy, and B. Iván, *Polym. Bull.*, **3**, 339 (1980).
12. J. P. Kennedy, L. R. Ross, and O. Nuyken, *Polym. Bull.*, **5**, 5 (1981).
13. V. S. C. Chang and J. P. Kennedy, *Polym. Bull.*, **9**, 518 (1983).
14. V. S. C. Chang and J. P. Kennedy, *Polym. Bull.*, **4**, 513 (1981).
15. P. J. Flory and J. Rehner, Jr., *J. Chem. Phys.* **11**, 521 (1943).
16. B. E. Eichinger and P. J. Flory, *Trans. Faraday Soc.*, **64m**, 2035 (1968).
17. Kurt Frisch Sr., private communication.
18. F. Bueche, *J. Polym. Sci.*, **24**, 189 (1957).

Received June 11, 1986
Accepted October 18, 1986